JAUES

INVESTIGATIONS OF THERMAL COMFORT AND AIR FLOW DISTRIBUTION IN NATURALLY VENTILATED LIVING ROOM WITH A CEILING FAN

Ahmed El Degwy[1,*], Ahmed Aboulmagd[2]

Mechanical Power Engineering Department, Faculty of Engineering, Cairo University, Giza 12613, Egypt

*Corresponding: mpdfoecu_ahmed@cu.edu.eg

ABSTRACT

In this paper, numerical analysis is used to investigate thermal comfort and airflow patterns in ventilated living rooms, including window openings and utilizing a ceiling fan. The air distribution in the living room was accurately predicted in this study using the CFD program. A five-bladed commercial ceiling fan is used to ventilate the room. The major goal of this study is to change the fan speed, fan height, and fan direction of rotation for the purpose of providing the thermal comfort conditions for individuals in the living room. Temperatures, velocities, the PPD index (Predicted Percentage Dissatisfied), and the PMV index (Predicted Mean Vote) distribution have all been taken into consideration while analyzing each case. The results showed that the best thermal comfort values are associated with fan placement in the center of the room at a height of 2.75 m from the floor at a rotational speed of 110 rpm. The overall level of thermal comfort is not significantly different whether downward-drive or upward-drive fans are used, but there is a substantial variation in the local level of thermal comfort in an occupied zone.

Keywords: Fan; CFD; Thermal Comfort; PPD; PMV.

تحقيق في الراحة الحرارية وتوزيع تدفق الهواء في غرفة معيشة ذات تهوية طبيعية مع مروحة سقف

أحمد الدجوي[1]* ، أحمد ابوالمجد[1]

¹ قسم هندسة القوى الميكانيكية, كلية الهندسة, جامعة القاهرة, ص. ب ١٢٦١٣, مصر

* البريد الإلكترونى للمؤلف الرئيسى: mpdfoecu_ahmed@cu.edu.eg

الملخص

في هذا البحث ، يتم استخدام التحليل العددي للتحقق من الراحة الحرارية وأنماط تدفق الهواء في غرف المعيشة ذات التهوية بما في ذلك فتحات النوافذ مع استخدام مروحة السقف. تم التنبؤ بدقة بتوزيع الهواء في غرفة المعيشة في هذه الدراسة باستخدام برنامج تحليل عددى (CFD). تستخدم مروحة سقف تجارية بخمس شفرات لتهوية الغرفة. الهدف الرئيسي من هذه الدراسة هو تغيير سرعة المروحة وارتفاعها واتجاه دوران المروحة لغرض توفير ظروف الراحة الحرارية للأفراد في غرفة المعيشة. تم أخذ توزيع درجات الحرارة والسرعات ومؤشر PPD (النسبة المئوية المتوقعة غير الراضية) ومؤشر PMV (متوسط التصويت المتوقع) في الاعتبار أثناء تحليل

INVESTIGATIONS OF THERMAL COMFORT AND AIR FLOW DISTRIBUTION IN NATURALLY VENTILATED LIVING ROOM WITH A CEILING FAN

كل حالة. أظهرت النتائج أن أفضل قيم الراحة الحرارية مرتبطة بوضع المروحة في وسط الغرفة على ارتفاع ٢,٧٥ متر من الأرضية، بسرعة دوران ١١٠ دورة في الدقيقة. لا يختلف المستوى العام للراحة الحرارية اختلافًا كبيرًا سواء تم استخدام مراوح الدفع إلى الأسفل أو الدفع لأعلى ، ولكن هناك تباينًا كبيرًا في المستوى المحلي للراحة الحرارية في منطقة مشغولة.

1. INTRODUCTION

Many individuals in underdeveloped nations may not have access to an air conditioning system to provide comfortable temperatures in areas. Instead, ceiling fans are used in homes and workplaces. These fans are affordable, easy to construct, simple to install, and require minimal maintenance. The air is moved by the ceiling fan to alter the air's composition and replace it with new air. In order to disinfect the air in the rooms, it is also utilized to circulate the air on sterilizers. Ceiling fans are also utilized in air-conditioned spaces to enhance the uniform dispersion of conditioned air [1]. The ceiling fan successfully cools people by adding gradual movement to the hot air in the room, reducing evaporation. It turns considerably more slowly than an electric desk fan. Unlike air conditioning equipment, fans do not produce any air, yet they consume significantly less energy (refrigeration air charged with thermodynamics). A ceiling fan may be used to reduce the hot air compartmentalization of the space, increasing energy efficiency in temperature control by pushing it to affect the impression of both the readings and the thermostat readings. Offices, factories, and industries typically employ commercial or industrial roof fans. Most commercial and industrial ceiling fans come with three blades and a high-speed motor. However, some can be discovered with more than three blades. In contrast to other ceiling fan kinds, these energy-saving ceiling fans typically provide enormous quantities of airflow. Industrial ceiling fans with metal blades were ubiquitous in American homes in the 1980s, although industrial fans used in domestic settings are still prevalent in the Middle East today. The direction and velocity of flow affect the efficacy of the upper-room ultraviolet germicidal irradiation (UR-UVGI) system's ability to disinfect, according to Zhu et al. [2]. A parametric investigation on the effects of running a ceiling fan in an air-conditioned setting was done by Son et al. [3]. When the fan's normal air speed was raised, thermal comfort was found to move noticeably toward the cooler end of the temperature range. The impact of utilizing a ceiling fan in addition to an air conditioner on people's thermal comfort was investigated by Son et al. [4]. They discovered that thermal comfort is highly reliant on the placement of the input diffuser, whether it is used frequently or infrequently as a ceiling fan. On the other hand, thermal comfort is substantially influenced by the fan's vertical air speed. The effectiveness of upper-room ultraviolet germicidal irradiation (UVGI) was statistically examined by George Pichurov et al. [5] in a space with a ceiling fan that rotated at three different speeds and blasted air upwards or downward. They discovered that the UVGI system worked best when the fan was blowing upward. In order to analyse temperature dynamics in a cold storage and investigate the impact of cooling management on quality change and energy use, Gruyters et al. [6] created a transient CFD model. In their brief assessment of frequently used ceiling fan models from Krole et al. [7] identified various issues with model choice. Chen et al. [8] examined how several characteristics affected the dispersion of air. It was discovered that the impacted cylindrical area is the sole place where air velocity is altered. Attention has been drawn to a hybrid ventilation system that blends mechanical and natural ventilation because of its affordable running costs and consistent ventilation rate. By contrasting a ventilation system's operation with that of a ceiling fan, the application of hybrid ventilation techniques in building design is advanced by this work. The airflow characteristics of ceiling fans and their impact on thermal comfort were investigated using numerical research. Following model validation [9], Investigation is done into how the supply air velocity and blade pitch affect the flow and thermal field. Additionally, ceiling fans used with air conditioners improve thermal comfort while consuming less energy. Understanding the right

flow field around a rotating ceiling fan will help designers create fan blades that are more energy-efficient, which may save a lot of money on energy costs. For this reason, varieties of turbulence models are available, and each would forecast some situations more correctly than others would. The Spalart Allmaras (SA) model was shown to be the most accurate when analyzing experimentally collected data [10]. A comprehensive analysis of the literature on ceiling fans summarizes what is known about its consequences and what will be needed moving forward. The most thoroughly researched metrics among the several consequences of ceiling fans for interior spaces, according to the findings, are thermal comfort and airflow. Findings point to a knowledge gap on the effects of hybrid ventilation, which combines Effects of ceiling fans and natural ventilation on interior air quality (IAQ) [11]. When windows are opened in a larger space, the air velocity becomes less uneven, falling from 76% to 39%. Regularly opening windows and utilizing ceiling fans to generate air movement can improve the air distribution in the room. Designers can raise comfort levels by considering patterns of non-uniform airflow when deciding the number and location of fans and windows [12].

It is clear from [11] that there is a need for larger and deeper studies of the use of fans in different applications. As far as the authors are aware, no previous specialized studies in the associated literature have addressed the thermal comfort in living rooms [11]. The purpose of the current study is to make and validate a 3D fan model that is frequently used to move air in a room in a typical location as well as to investigate the influence of air movement on thermal comfort within the space.

2. MATERIALS AND METHODS

2.1. MATHEMATICAL MODELING

The flow field under investigation is 3D and compressible under transient conditions. With the help of the CFD modelling strategy used in this work, the four main governing equations required to solve the flow problem are the continuity, the momentum, energy, and species equations as follows [13]:

$$\frac{\partial \rho}{\partial t} + \nabla \cdot (\rho \vec{v}) = 0 \tag{1}$$

$$\frac{\partial (\rho \vec{v})}{\partial t} + \nabla \cdot \rho \vec{v} \vec{v} = -\nabla P + \nabla \cdot (\bar{\bar{\tau}}) + \rho \vec{g} \tag{2}$$

$$\frac{\partial (\rho E)}{\partial t} + \nabla \cdot (\vec{v}(\rho E + P)) = \nabla \cdot (\rho k_{eff} \nabla T - h + (\bar{\bar{\tau}}_{eff} \cdot \vec{v})) \tag{3}$$

$$E = h - \frac{P}{\rho} + \frac{v^2}{2} \tag{4}$$

Where ρ is the air density (kg/m³), v is velocity (m/s), t is the time in second, P is the local air pressure (Pa), $\bar{\bar{\tau}}$ is the stress tensor (Pa), k_{eff} is the effective thermal conductivity (W/m.K), h is the enthalpy (J/kg), E is the total energy (J), T is the air temperature (K), and $\vec{g}$ is the gravitational acceleration (m/s²).

For H_2O, distribution of species concentrations was also investigated eq. (5).

$$\frac{\partial(\rho \vec{v} C_i)}{\partial t} = -\nabla \cdot \vec{J_i} + S_i \tag{5}$$

$$\vec{J_i} = -\rho D_{i,m} \nabla Y_i - D_{T,i} \frac{\nabla T}{T} \tag{6}$$

where Y_i is the mass fraction, $\vec{J_i}$ is the diffusion flux and $D_{i,m}$ is the mass diffusion coefficient of the ith species. $D_{T,i}$ is the Soret diffusion coefficient, and S_i is the source term.

The turbulence effect is taken into consideration by using the two-equation, k-ε model, which predicts the turbulence viscosity dependent on the kinetic energy of the turbulence and how it dissipates. The Prandtl-Kolmogorov equation states that the turbulent viscosity in this model is connected with the dissipation rate, ε, and the kinetic energy, k, of the turbulence, according to [13].

$$\mu_t = \frac{C_\mu \rho k^2}{\varepsilon}, where\ C_\mu = 0.09 \tag{7}$$

The definitions of total thermal comfort used to evaluate the thermal environment inside the living room are provided in this section. The prediction mean vote (PMV), expected percent of dissatisfaction (PPD). PMV measures the thermal sensitivity of the human body to hot and cold on a scale from +3.0 (very hot) to -3.0 (very cold). When PMV gets close to zero, people inside tend to feel more comfortable. To accommodate sleeping settings, Lin and Deng [14] updated the Fanger's model, a well-known measure of thermal comfort. Their model is stated as follows:

$$PMV = 0.09982 \times \left\{40 - \frac{1}{B}\left[\left(34.6 - \frac{4.7T_r + h_c T_{ma}}{4.7 + h_c}\right) + 0.37623 \times (5.52 - P_v)\right]\right\} \tag{8}$$
$$- 0.09979 \times [0.0562 \times (34 - T_{ma}) + 0.692 \times (5.87 - P_v)]$$

where P_v water vapour pressure in humid air, h_c is the coefficient of convective heat transfer., which is computed depending on the speed of the air (v), and T_r and T_{ma} are the average radiant temperature and the average room temperature, respectively.

$$h_c = \begin{cases} 5.1 \left[\frac{W}{m^2}.K\right] & for\ 0.00 < v < 0.15 \frac{m}{s} \\ 2.7 + 8.7\ v^{0.669} \left[\frac{W}{m^2}.K\right] & for\ 0.15 < v < 1.50 \frac{m}{s} \end{cases} \tag{9}$$

Because of a predetermined clothing factor of 0.5 clo, the thermal resistance of the seating arrangement (B) is assumed 0.261655 m^2.K/W. The percentage of unsatisfied occupants subjected to the same heat environment is quantified by PPD [14], [15]. It is directly connected to PMV in the way as follows:

$$PPD = 100 - 95 \times \exp(-0.03352 \times PMV^4 - 0.21792 \times PMV^2) \tag{10}$$

[(-0.5) ≤ PMV ≤ (0.5) satisfied range] is the recommended range under ISO 7730 [16].

2.2. GRID GENERATION

ANSYS ICEM-CFD was used to make the surface model. Accurate mesh in the form of an MSH file were produced using surface geometry produced by the ICEM-CFD program. The flow equations need to be solved, the mesh file was sent to FLUENT and the proper flow boundary conditions were applied. The field matrix equations were solved using FLUENT, and the results were visualized using FLUENT deployment. By resolving the flow domain of four meshes topologies with 1,130,500, 2,200,000, 3,670,000, and 5,400,000 cells, respectively, the mesh dependence was investigated. The results revealed that the maximum speed of the coarse mesh and the finer mesh varied by 7.65% and 0.5%, respectively, between the two finer meshes, respectively. The mesh is particularly dense next to the fan blades and progressively gets bigger until it reaches 0.05 m in the rest of the room.

2.3. VALIDATION

Comparing the observed and simulated values at 24 points in a plane 0.15 m above the ground has been done as validation [17]. To assess the reliability and applicability of the existing CFD model, a comparison was made. The simulation uses the common standard k-ε turbulence model, and the outcomes are contrasted with the measured findings [17], as shown in figure 1. Results demonstrate that there are variances at certain points and also at some locations in the planes where measured and simulated values are identical. The measurement devices inherent error rate, we can infer, is to blame for this occurrence. However, the numerical numbers are within a reasonable range and show the same pattern.
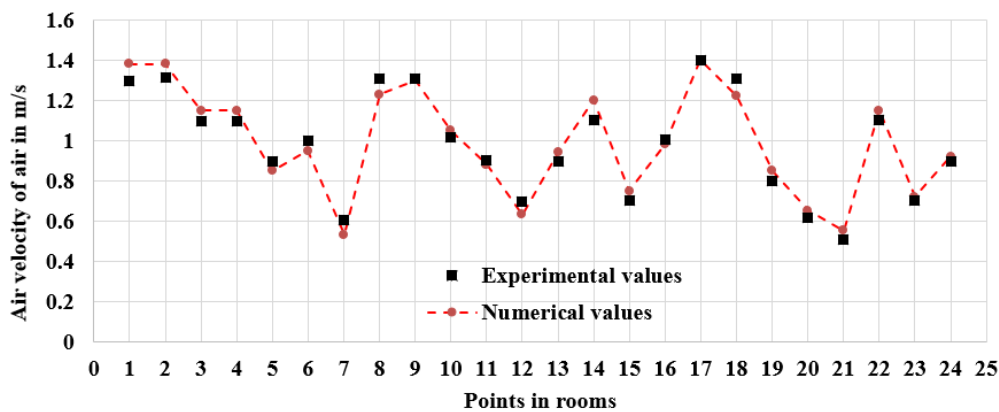

Fig. 1: Comparison of the experimental and numerical at 0.15 m of height from the floor

2.4. NUMERICAL SOLUTION STABILITY

The relaxation factor, which controls the resolution of the solution for each repeat, and the segment's remaining value, which controls when the repeat process can be stopped, are the two important repetition parameters before the simulation is started. Due to the high number of Riley and the variation in solution, relaxation factors were used to increase the stability of the solution. The SIMPLE technique was applied to link the velocity and pressure flow fields. When the relative inaccuracy of the energy equation was less than 10^{-7} and that of the other solved equations was less than 10^{-4}, iterations were halted. The computation takes place with a 0.05-second time step for 110 rpm and 0.1-second for the other rpm. The solution begins in Steady State with the fan turned off, then switches to Transient with the fan on. The surface-to-surface radiation model (S2SM) was also used in the current investigation [15].

3. CASE STUDY DESCRIPTION

Figure 2 displays the investigational living room model. Its dimensions are (length × width × height) (6 m × 4 m × 3. 5 m). As illustrated in Fig.2, the fan it is fixed on the ceiling, and placed in the center of the ceiling space at three different heights: 2.75, 3.00, and 3.25 m from the finished floor.
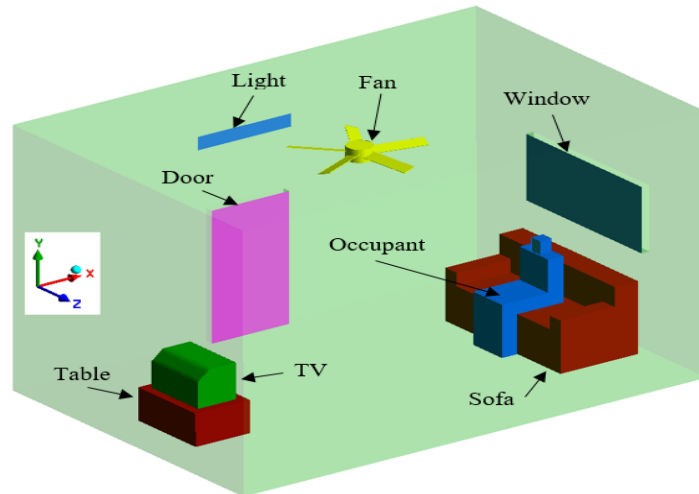

Fig. 2: Layout of the living room under investigation

3.1. FAN DESCRIPTIONS

The model for the axial 5-blade ceiling fan has a revolving reference frame that has a 152.0 cm diameter. This radius should be as large as is practical without crossing any spinning surfaces. In figure 3, this is depicted.
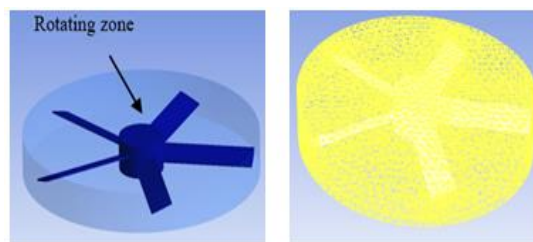

Fig. 3: Layout of axial 5-blade ceiling fan under investigation

3.2. OCCUPANTS MODELLING

With the aid of ANSYS ICEM-CFD, the mesh is produced. The occupant was modelled as a combined volume made up of a cube for the head and a rectangle for the body, arms, and legs. Figure 4 depicts the characteristics and measurements of an occupant. The seated occupant's primary measurements are (length × width × depth) (1.30 x 0.60 x 0.25) m.

Fig. 4: The configuration of an occupant

The gases exhaled by the occupant had a temperature of 37 °C and a velocity of 0.3 m/s, and were assumed to be consisting of air, CO_2, and water. The person's nose served as their egress. The bulk of the expelled gases, with mass fractions of 0.043 and 0.05, respectively, were composed of H_2O and CO_2 [18]. The nose's dimension is (0.05 m x 0.02 m).

3.3. BOUNDARY CONDITIONS

The room's walls, furniture, and other non-heat-dissipating components were all adjusted to have zero wall heat fluxes. It is assumed that the body has no diffusive flux and that it is considered as a wall at a constant temperature, which is 32.5 °C skin temperature [19]. The air relative humidity and temperature in the room is 40% and 28 °C respectively. 24 cases are investigated under this study, depending on fan speed (40, 50, 60, 110 rpm), fan blade angle fixed at 30º and fan height from the ground (3, 3.25, 3.5 m). In this investigation, it was assumed that the ambient air temperature was always 28 °C. Table 1 demonstrates the values of the heat sources in the living room.

Table 1: Boundary conditions of the living room [19]

Heat Source Name	Heat Flux W/m²	Amount
Fluorescent lamp	50	1
Television	80	1
Human body	60	1

4. RESULS AND DISCUSSIONS

In order to select the optimum design scenario for the living room naturally ventilated with ceiling fan among those taken into consideration in this study, an analysis of the airflow pattern, thermal comfort, and temperature distribution is included in this comparative study.

4.1. CEILING FAN IN DOWNWARD FLOW MODE AT A HEIGHT OF 3.25 M

Figure 5 displays the air velocities within the living room at various fan speeds at a horizontal level of Y = 1 m from the room floor. Additionally, Figure 5 demonstrates that every increase in fan speed increases air velocity in the living room, mainly under the fan, which improves thermal comfort, but within limit. When moving downward, the fan draws air from the top and pushes it to the bottom in circular swirls that begin with a diameter equal to the fan blades and get bigger as we get closer to the room's floor. The air is swiftly propelled by the fan blades at first, but as we travel farther from them

toward the room's floor, the air speed slows down. The arrangement of the furniture and the airflow coming through the window apertures both have an impact on the uneven distribution of the airflow. Additionally, Figure 5 further shows that the average air speed under the fan is 0.4 m/s while the fan blades are rotating at a rate of 40 rpm at a distance of $Y = 1$ m from the room's floor, and the air speeds are 0.6, 0.75, and 2.0 m/s, respectively, for fan blade speeds of 50, 60, and 110 rpm. The air speed next to the person sitting on the sofa is at an acceptable level, except in the case of the fan speed of 110 rpm, which is high.
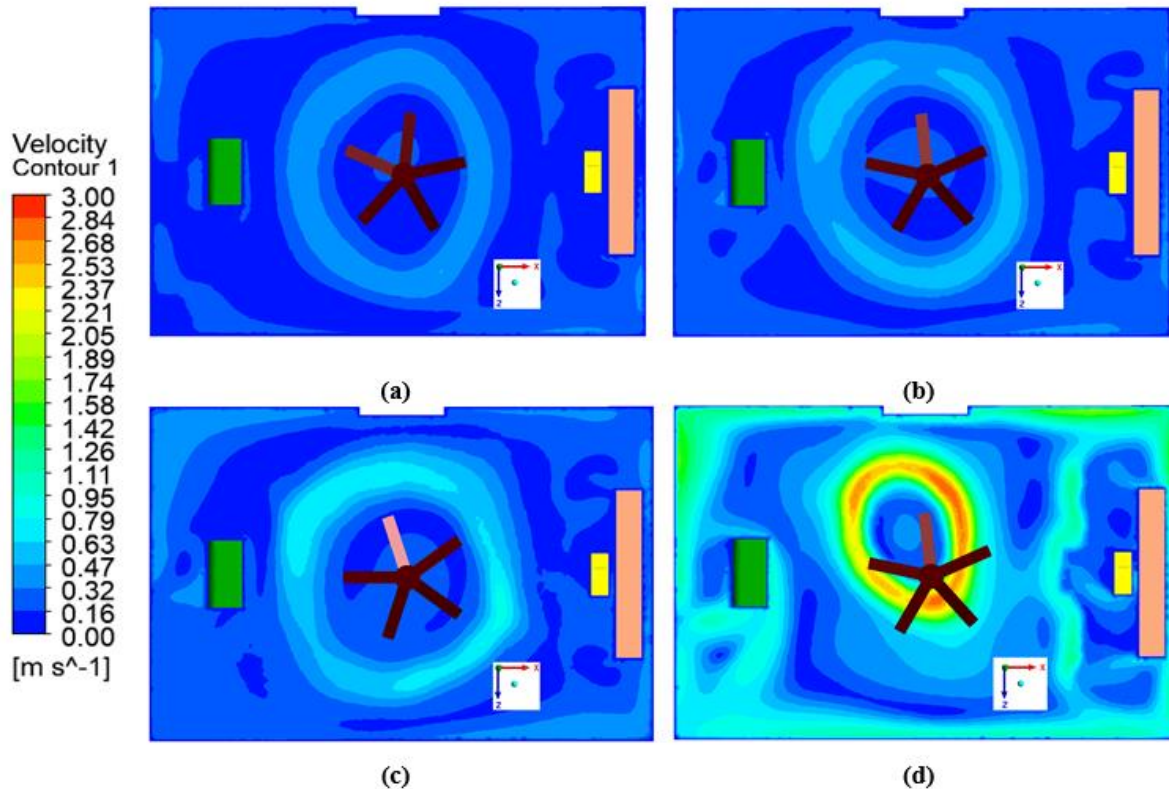

Fig. 5: Air speed contours (m/s) at horizontal plane (Y = 1.0 m), after 15 minutes:

(a) N = 40 rpm, (b) N = 50 rpm, (c) N = 60 rpm, (d) N = 110 rpm

Figure 6 shows that the air temperature in the room is equally distributed at roughly 28 °C, notably near the window, and rises to 40 °C surrounding the heating source (television). The distribution of temperatures inside the room depends on the airflow pattern coming from the fan and window, as well as on the location of the heating source inside the room. Additionally, it was discovered that if the fan was working at high speeds, it might cause thermal discomfort by dispersing the heat from the TV in the direction of the person seated on the sofa. The open window behind the person seated on the sofa helps to circulate fresh air throughout the space, lowering the temperature and humidity levels while providing thermal comfort.
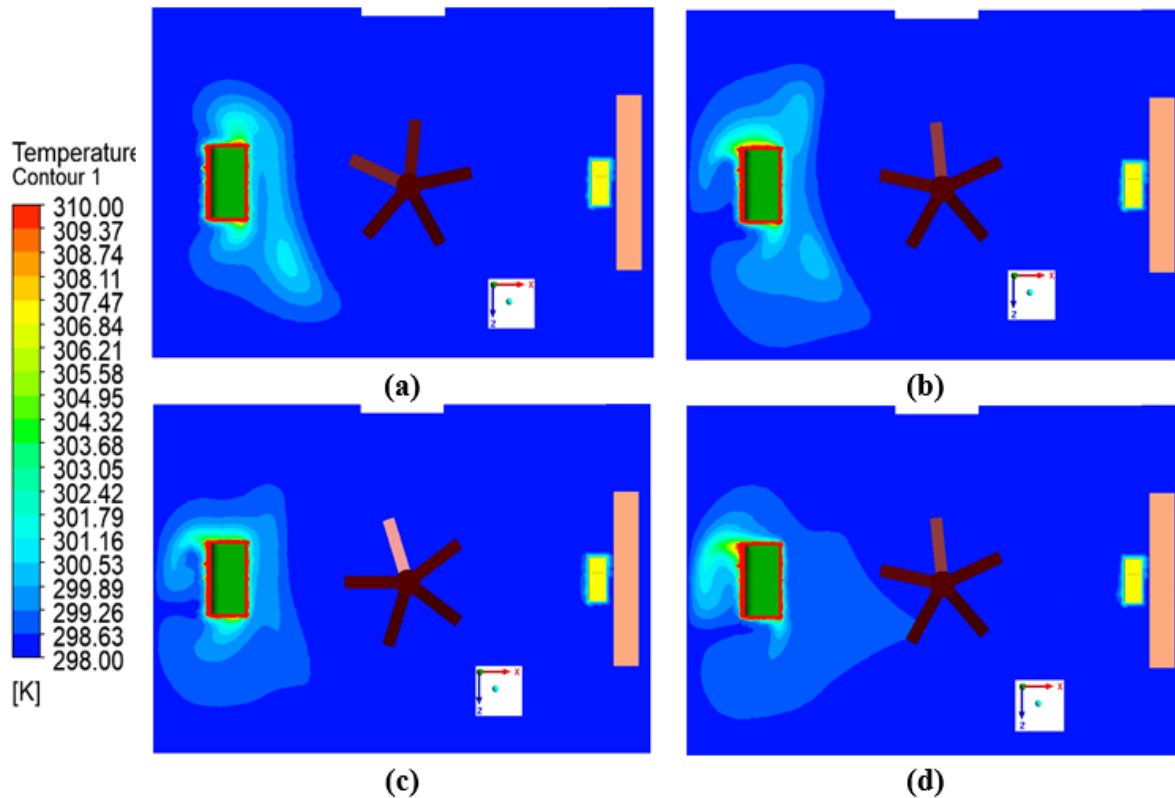
Fig. 6: Air temperature contours (m/s) at horizontal plane (Y = 1.0 m), after 15 minutes:

N = 40 rpm, (b) N = 50 rpm, (c) N = 60 rpm, (d) N = 110 rpm

4.2. CEILING FAN IN UPWARD FLOW MODE AT A HEIGHT OF 3.25 M

Figure 7 displays the air velocities within the living room at various fan speeds at a horizontal level of Y = 1 m from the room floor. Additionally, Figure 7 demonstrates that every increase in fan speed increases air speed in the living room. It is clear that in the case of the upward thrust of the fan, the air is pulled from the bottom and pushed up towards the ceiling, and the phenomenon of the *coanda effect* occurs, which is the air that sticks to the ceiling until it catches up with the walls of the room due to the effect of the viscosity as well as the energy of air movement, can see that in figure 9. The fan blades push the air quickly at first, but as we move away from them towards the ceiling of the room, the air speed slows down to the walls of the room. Additionally, it can be observed that the distribution of velocities inside the space is better and that they are at comfortable thermal velocities. Also, the velocity is 0.15 m/s while the fan blades are rotating at a rate of 40 RPM at a distance of Y = 1 m from the room's floor, and the air speeds are 0.25, 0.3, and 0.46 m/s, respectively, for fan blade speeds of 50, 60, and 110 RPM. The air speed next to the person sitting on the sofa is at an acceptable level, except in the case of the fan speed of 110 rpm, which is high.
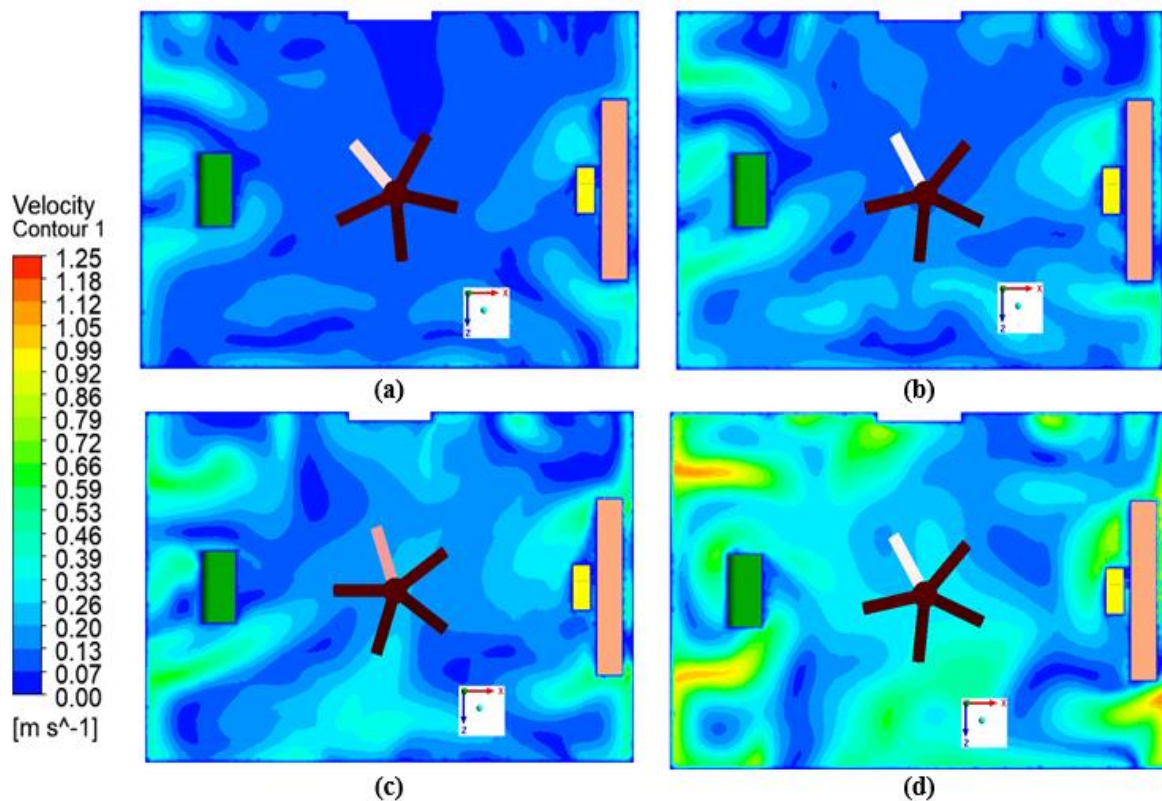
Fig. 7: Air speed contours (m/s) at horizontal plane (Y = 1.0 m), after 15 minutes:

N = 40 rpm, (b) N = 50 rpm, (c) N = 60 rpm, (d) N = 110 rpm

Figure 8 shows that the temperature in the room is equally distributed at roughly 26 ºC, notably near the window, and rises to 40 ºC surrounding the heating source (television). The distribution of temperatures inside the room depends on the airflow pattern coming from the fan and window, as well as on the location of the heating source inside the room. Besides, it is also clear in the case of the upward thrust of the fan that there is better heat distribution due to the good airflow pattern inside the room. The open window behind the person seated on the sofa helps to circulate fresh air throughout the space, lowering the temperature and humidity levels while providing thermal comfort.

Figure 9 provides an evident that in the case of the forward thrust of the fan, a recirculation zone forms between the room's walls and the air curtain coming from the fan. As a result, the air does not change well in this area, and a person seated on the couch may have thermal discomfort. But in the case of the upward thrust of the fan, solves this problem. It is clear that in the case of the upward thrust of the fan, the air is pulled from the bottom and pushed up towards the ceiling, and the phenomenon of the *coanda effect* occurs, which is the air that sticks to the ceiling until it catches up with the walls of the room due to the effect of the viscousity as well as the energy of air movement.
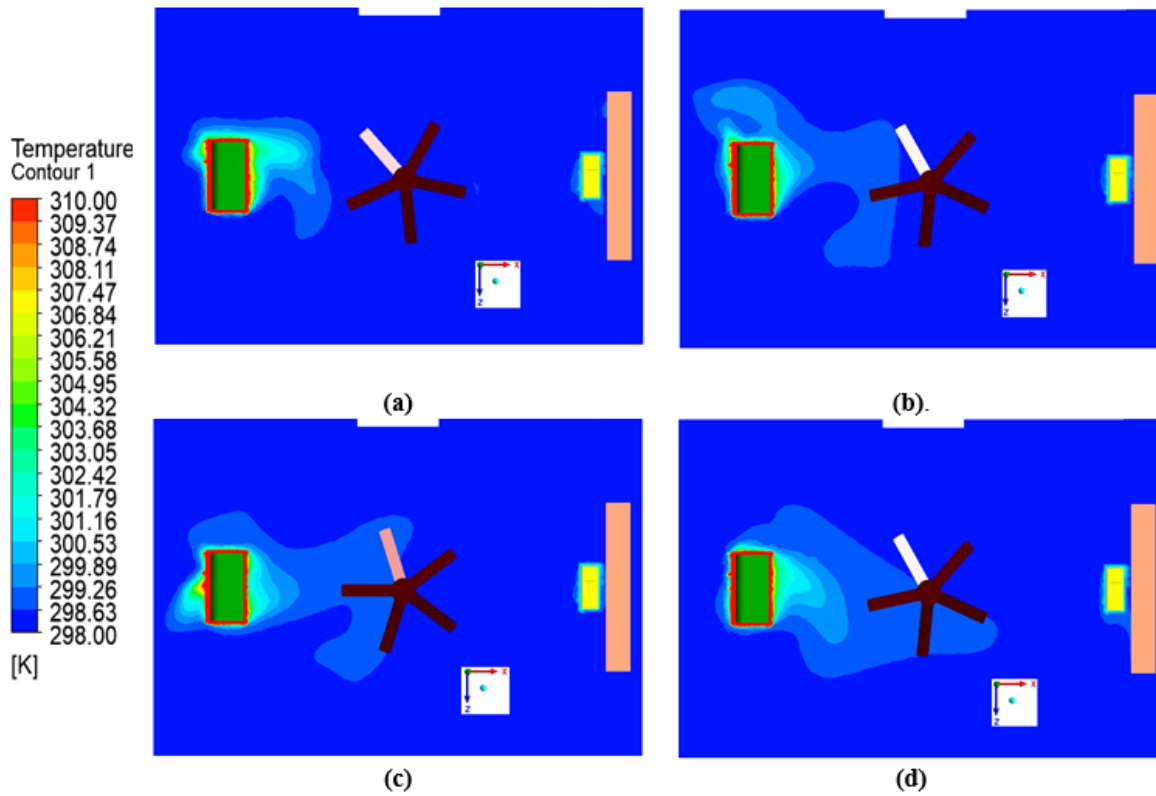
**Fig. 8: Air temperature contours (m/s) at horizontal plane (Y = 1.0 m), after 15 minutes: (a) N = 40 rpm,
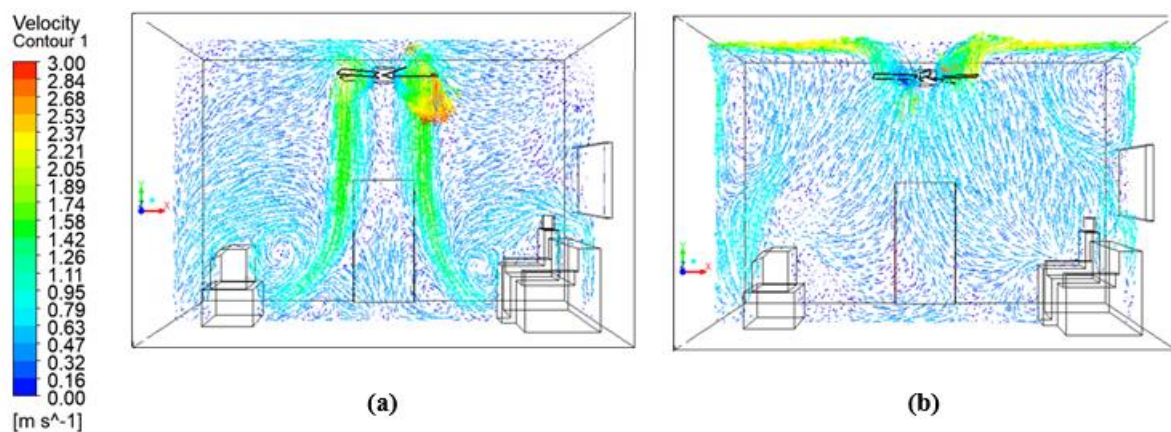(b) N = 50 rpm, (c) N = 60 rpm, (d) N = 110 rpm**

**Fig. 9: Velocity vectors colored by velocity magnitude (m/s) at vertical plane (Z = 2.0 m), after 15 minutes:
(a) 60 rpm, forward fan flow, (b) 60 rpm, backward fan flow**

INVESTIGATIONS OF THERMAL COMFORT AND AIR FLOW DISTRIBUTION IN NATURALLY VENTILATED LIVING ROOM WITH A CEILING FAN

In table 2 and 3, it is obvious that PMV values range is from (0.89 to 0.43) and in other cases, it is significantly above the permitted level cases. [(-0.5) ≤ PMV ≤ (0.5) satisfied range] is the recommended range under ISO 7730 [16]. Also, in table 2 and 3 shows that PPD values in the most of the cases is slightly higher than the acceptable range according to standard ISO7730 [16] recommends (PD ≤ 10%). According to table 3 and 4, the best thermal comfort values are when the fan is placed in the center of the room at a height of 2.75 m from the floor, and when its rotation speed is 110 rpm.

Tables 2 and 3 demonstrate the values of PPD and PMV of the living room at different heights in the case of downward and upward fan mode. The overall level of thermal comfort is not significantly different whether downward-drive or upward-drive fans are used, but there is a substantial variation in the local level of thermal comfort in an occupied zone.

Table 2: PPD and PMV inside the living room in case of a downward airflow mode.

1- At height = 2.75 m	PPD	PMV
0 rpm	53.62	1.55
40 rpm	15.91	0.72
50 rpm	14.15	0.66
60 rpm	12.30	0.59
110 rpm	9.42	0.46
2- At height = 3.00 m		
40 rpm	20.25	0.85
50 rpm	18.16	0.79
60 rpm	15.91	0.72
110 rpm	13.33	0.63
3- At height = 3.25 m		
40 rpm	22.49	0.91
50 rpm	19.18	0.82
60 rpm	17.49	0.77
110 rpm	13.87	0.65

Table 3: PPD and PMV inside the living room in case of an upward airflow mode.

1- At height = 2.75 m	PPD	PMV
40 rpm	15.61	0.71
50 rpm	13.60	0.64
60 rpm	11.33	0.55
110 rpm	8.86	0.43
2- At height = 3.00 m		
40 rpm	19.53	0.83
50 rpm	17.49	0.77
60 rpm	15.31	0.70
110 rpm	12.55	0.60
3- At height = 3.25 m		
40 rpm	21.72	0.89
50 rpm	18.50	0.80
60 rpm	16.84	0.75
110 rpm	13.07	0.62

5. SUMMARY AND CONCLUSIONS

The thermal comfort and flow pattern of a living room have been studied in this work using numerical CFD modelling. Using commercial software with a grid size bigger than 5 million control volumes, a typical 5-blade ceiling fan was simulated. The acquired findings demonstrate the calculating method's sensitivity to the fan arrangement and easily produce the flow patterns downstream of the fan. The right combination of fan speeds and its location results in good airflow and a high level of thermal comfort. Due to the effect of air velocity on occupants, low fan rotation speed discharge is appropriate for low-ceiling rooms, whereas high fan rotation speed is appropriate for high-ceiling rooms. Because this study concentrated on the relatively high ceilings that are common in older buildings, the impact of fans should also be investigated in living rooms with low ceilings. When the fan is running at high speeds, more evaporation of body perspiration occurs, which increases the feeling of thermal comfort, but this also depends on the humidity inside the living room. The temperature of the air that the fan pushes depends heavily on the ambient air, the temperature of the ceiling in the living room, and the heat load present inside the room. The arrangement of the furniture and the airflow coming through the window apertures both have an impact on the uneven distribution of the airflow. According to this study, the best thermal comfort values are when the fan is placed in the center of the room at a height of 2.75 m from the floor and when its rotation speed is 110 rpm. The overall level of thermal comfort is not significantly different whether downward-drive or upward-drive fans are used, but there is a substantial variation in the local level of thermal comfort in an occupied zone.

INVESTIGATIONS OF THERMAL COMFORT AND AIR FLOW DISTRIBUTION IN NATURALLY VENTILATED LIVING ROOM WITH A CEILING FAN

REFERENCES

[1]   A. ElDegwy and E. E. Khalil, "Simulation of air flow pattern in a room with ceiling mounted circulator," 2017. doi: 10.2514/6.2017-1996.

[2]   S. Zhu, J. Srebric, S. N. Rudnick, R. L. Vincent, and E. A. Nardell, "Numerical investigation of upper-room UVGI disinfection efficacy in an environmental chamber with a ceiling fan," *Photochem. Photobiol.*, vol. 89, no. 4, pp. 782–791, 2013, doi: 10.1111/php.12039.

[3]   S. H. Ho, L. Rosario, and M. M. Rahman, "Thermal comfort enhancement by using a ceiling fan," *Appl. Therm. Eng.*, vol. 29, no. 8–9, pp. 1648–1656, 2009, doi: 10.1016/j.applthermaleng.2008.07.015.

[4]   S. H. Ho, L. Rosario, and M. M. Rahman, "Effect of using ceiling fan on human thermal comfort in air-conditioned space," *Collect. Tech. Pap. - 3rd Int. Energy Convers. Eng. Conf.*, vol. 3, no. August, pp. 1831–1841, 2005, doi: 10.2514/6.2005-5734.

[5]   G. Pichurov, J. Srebric, S. Zhu, R. L. Vincent, P. W. Brickner, and S. N. Rudnick, "A validated numerical investigation of the ceiling fan's role in the upper-room UVGI efficacy," *Build. Environ.*, vol. 86, pp. 109–119, 2015, doi: 10.1016/j.buildenv.2014.12.021.

[6]   W. Gruyters, P. Verboven, M. Delele, S. G. Gwanpua, A. Schenk, and B. Nicolaï, "Évaluation Numérique Des Stratégies De Refroidissement Par Régulation Tout Ou Rien Adaptatives Pour Économiser De L'Énergie Durant Le Stockage À Long Terme Des Pommes," *Int. J. Refrig.*, vol. 85, pp. 431–440, 2018, doi: 10.1016/j.ijrefrig.2017.10.018.

[7]   A. Król and M. Król, "Study on numerical modeling of jet fans," *Tunn. Undergr. Sp. Technol.*, vol. 73, no. October 2017, pp. 222–235, 2018, doi: 10.1016/j.tust.2017.12.024.

[8]   W. Chen *et al.*, "Experimental and numerical investigations of indoor air movement distribution with an office ceiling fan," *Build. Environ.*, vol. 130, no. November 2017, pp. 14–26, 2018, doi: 10.1016/j.buildenv.2017.12.016.

[9]   M. Alizadeh and S. M. Sadrameli, "Numerical modeling and optimization of thermal comfort in building: Central composite design and CFD simulation," *Energy Build.*, vol. 164, pp. 187–202, 2018, doi: 10.1016/j.enbuild.2018.01.006.

[10]   D. Casseer and C. Ranasinghe, "Assessment of Spallart Almaras Turbulence Model for Numerical Evaluation of Ceiling Fan Performance," *MERCon 2019 - Proceedings, 5th Int. Multidiscip. Moratuwa Eng. Res. Conf.*, pp. 577–582, 2019, doi: 10.1109/MERCon.2019.8818888.

[11]   S. Omrani, S. Matour, K. Bamdad, and N. Izadyar, "Ceiling fans as ventilation assisting devices in buildings: A critical review," *Build. Environ.*, vol. 201, no. February, p. 108010, 2021, doi: 10.1016/j.buildenv.2021.108010.

[12]   T. K. Jayasree, B. S. Jinshah, and T. Srinivas, "The effect of opening windows on the airflow distribution inside naturally ventilated residential bedrooms with ceiling fans," *Build. Serv. Eng. Res. Technol.*, vol. 43, no. 1, pp. 23–39, 2022, doi: 10.1177/01436244211024084.

[13]   A. E. A. E. Degwy, S. M. Morkos, A. S. Sabry, and E. E. Khalil, "Numerical computations of flow regimes in enclosed spaces," *Proc. ASME Des. Eng. Tech. Conf.*, vol. 5, no. 2, pp. 817–824, 2012, doi: 10.1115/DETC2012-70285.

[14]   Z. Lin and S. Deng, "A study on the thermal comfort in sleeping environments in the subtropics-Developing a thermal comfort model for sleeping environments," *Build. Environ.*, vol. 43, no. 1, pp. 70–81, 2008, doi: 10.1016/j.buildenv.2006.11.026.

[15]   A. Eldegwy and E. E. Khalil, "Passengers' thermal comfort in private car cabin in hot climate," *2018 Jt. Propuls. Conf.*, pp. 1–11, 2018, doi: 10.2514/6.2018-4613.

[16]   "ISO - ISO 7730:2005 - Ergonomics of the thermal environment — Analytical determination and interpretation of thermal comfort using calculation of the PMV and PPD indices and local thermal comfort criteria." https://www.iso.org/standard/39155.html (accessed Jul. 11, 2022).

[17]   Y. Anand, S. K. Verma, and S. Anand, "Transient 3-D modelling of ceiling fan for achieving thermal comfort," *ASHRAE IBPSA-USA Build. Simul. Conf.*, pp. 197–204, 2018.

[18]   "American Society of Heating, Refrigeration, and Air-Conditioning Engineers, ANSI/ASHRAE 62: ventilation for Acceptable Indoor Air Quality, Atlanta, GA, ASHRAE, 2019

[19]   "R. and A.-C.E. (ASHRAE) The American Society of Heating, Thermal environmental conditions for human occupancy, Atlanta, GA; 2013.